**LA-UR** -84-3209

CONF-8405321--3

Los Alamos National Laboratory is operated by the University of California for the United States Department of Energy under contract W-7405-ENG-36



LA-UR--84-3209

DE85 002269

TITLE **FRONT TRACKING AND TWO DIMENSIONAL RIEMANN PROBLEMS: A CONFERENCE REPORT**

AUTHOR(S) James Glimm, Christian Klingenberg, Oliver McBryan, Bradley Plohr, David Sharp and Sara Yaniv

SUBMITTED TO To be published in the Proceedings of the Army Conference on Computers and Applied Mathematics, RPI, 1984.

MASTER



Los Alamos Los Alamos National Laboratory
Los Alamos, New Mexico 87545

# FRONT TRACKING AND TWO DIMENSIONAL RIEMANN PROBLEMS: A CONFERENCE REPORT

*James Glimm* [1, 3, 4, 6]
*Christian Klingenberg* [1, 4]
*Oliver McBryan* [1, 3, 5, 7]
*Bradley Plohr* [1, 3]
*David Sharp* [2, 8]
*Sara Yaniv* [1, 3, 4]

*ABSTRACT*

A substantial improvement in resolution has been achieved for the computation of jump discontinuities in gas dynamics using the method of front tracking. The essential feature of this method is that a lower dimensional grid is fitted to and follows the discontinuous waves. At the intersection points of these discontinuities, two-dimensional Riemann problems occur. In this paper we study such two-dimensional Riemann problems from both numerical and theoretical points of view. Specifically included is a numerical solution for the Mach reflection, a general classification scheme for two-dimensional elementary waves, and a discussion of problems and conjectures in this area.

## 1. Introduction

Many phenomena in nature are modeled by nonlinear hyperbolic systems of conservation laws:

$$u_t + \nabla \cdot f(u) = 0 . \tag{1.1}$$

The example considered here is the system of Euler equations for a compressible, inviscid, polytropic gas. The equation (1.1) represents an idealization. Its solutions are the limits, as viscosity parameters tend to zero, of the solutions of more complete equations such as the Navier-Stokes equations. The solutions of interest for the system (1.1) are frequently

1. Courant Institute of Mathematical Sciences, New York University, 251 Mercer Street, New York, N.Y. 10012.
2. Los Alamos National Laboratory, Los Alamos, N.M. 87545.
3. Supported in part by the Applied Mathematical Sciences subprogram of the Office of Energy Research, U.S. Dept. of Energy, Contract DE-A02-76ER03077.
4. Supported in part by the Army Research Office, Contract No. DAAG29-83-K-007.
5. Supported in Part by the National Science Foundation, Grant No. MCS-8207965.
6. Supported in part by the National Science Foundation, Grant No. MCS-8243730.
7. Alfred P. Sloan Foundation Fellow.
8. Supported by U.S. Department of Energy.

found to be piecewise smooth. For the Euler equations in one space dimension the jump discontinuities between the smooth pieces are contact discontinuities and shock waves. In two space dimensions these same wave modes give rise to surface singularities of codimension one. The Rankine-Hugoniot conditions, as derived from the integral form of the Euler equations, hold across these jumps.

When solving the system (1.1) numerically, the discontinuities that may occur in its solution may be resolved on coarser grids by the method of front tracking than by conventional finite difference methods. For two space dimensions, front tracking may be described as follows. A one-dimensional grid is placed onto the discontinuity. Its evolution in time is given by a two step procedure, using first the Rankine-Hugoniot relations to propagate the front normally and then using tangential equations to propagate surface waves. This approach works away from the points where the discontinuity curves meet. At such intersection points the geometry does not in general allow an operator splitting into normal and tangential directions, so the evolution of intersection points must be determined as the solution of a two-dimensional Riemann problem. To solve two-dimensional Riemann problems it is crucial to classify the coherent waves, which are defined to be dynamically stable intersection points of one-dimensional coherent waves. The region between the fronts is treated as an initial/boundary-value problem and is solved using (almost) standard finite difference methods. The front and interior schemes are connected in a strip $O(\Delta x)$ in width about the front. For a detailed description see [1].

The front tracking method appears to allow an increase of linear resolution by a factor of three or better, i.e. an improvement in the number of space-time computational grid units by a factor of 27 or better. The method has been tested on various problems. In Sec. 2 and 3 we compare the results of our numerical calculation to experimental results for two specific test problems. An example of how the motion of a two-dimensional coherent wave is determined numerically is given in Sec. 3. In Sec. 4 we give a classification of the two-dimensional coherent waves for compressible gas dynamics and indicate its derivation. In Sec. 5 we conclude with a discussion of outstanding questions related to Riemann problems.

## 2. Regular Reflection of Shock Waves

The front tracking scheme for two-dimensional gas dynamics has been tested on several problems that admit solution by other means. These problems are: an expanding or contracting circular shock followed by a contact discontinuity, the steady-state supersonic flow past a wedge, the Kelvin-Helmholtz instability, regular reflection of a shock wave, and Mach reflection of a shock wave. For details on the first five see [1].

In this section the numerical solution for nonsteady regular reflection of a shock wave is compared with experimental results [3]. The experiment consists of a planar shock (I) moving down a shock tube and impinging on a wedge with a sufficiently large

angle. When the incident shock strikes the wedge corner a reflected shock (R) is formed, which extends from the reflection point to the shock tube wall, where it forms a bow wave in front of the wedge, as shown in Fig. 2.1. We will refer to the region enclosed by the reflected shock as the "bubble". As with Riemann problems in general, the solution is self-similar, i.e $u(t,x) = u(\sigma t,\sigma x)$ for every $\sigma>0$. In the computation presented here, the Mach number of the incident shock is 2.05 and the angle of the wedge is 63.4°.

The numerical calculation was initialized just after the reflected shock had formed and enclosed only a small region about one quarter of a mesh interval in height. Data at the two ends of the reflected shock were obtained using a shock polar analysis. At the wedge corner, the two velocity components vanish. The remaining solution components at the corner and the full solution in the interior are determined by interpolation. One arbitrary parameter is used in the initialization, which is the oblateness of the bubble, defined as the ratio of the distance of the reflection point from the corner to the distance of the bow shock to the corner (the ratio of the lengths of the segments BC and AB in Fig. 2.1). The initial oblateness was taken from experimental data, but it can be determined approximately by a preliminary calculation because it is constrained to lie in a bounded interval by theoretical considerations. In fact the computational results are quite insensitive to its value. The initialization algorithm can be regarded as an approximate solution of the two-dimensional Riemann problem in a special case.

In Fig. 2.2 the contours of constant density and constant entropy that were obtained numerically are shown. In Fig. 2.3 the density distribution along the wall obtained from the calculation is superimposed on the experimental data.

### 3. Mach Reflection of Shock Waves

The intersection point of discontinuity curves will be called a node. In a neighborhood of a node the curves are approximated by straight lines separating wedge shaped regions. In analogy with the one-dimensional Riemann problem, we define a two-dimensional Riemann problem to be an initial value problem for a two-dimensional conservation law having data that is either a constant state or a simple rarefaction wave in each of a finite number of wedges. Such problems have been studied for scalar conservation laws [8,5,6], but only special solutions are known for systems of conservation laws. As with the solution of a one-dimensional Riemann problem, the solution of a two-dimensional Riemann problem will evolve into a more complicated configuration containing several elementary waves. Thus in front tracking we must solve a subcase of the full Riemann problem: determining the velocity and states associated with the one specific elementary wave (node) being tracked. We shall report in this section on a method for tracking the Mach node. Its propagation is a fully two-dimensional problem that cannot be be reduced to one-dimensional problems by spatial operator splitting. In fact successive solutions to one-dimensional problems still play a key role in solution of the Mach node, but their composition is governed by the geometry of the waves entering the node and not by an orthogonal set of coordinate axes.

Consider a planar shock moving down a shock tube and incident on a wedge with a small angle (see Fig. 3.1). In contrast with the regular reflection case we obtain a Mach reflection. The point where the incident (I) and the reflected shock (R) meet (the "Mach node") has lifted off the wall and is connected to the wall by a nearly straight shock called the Mach stem (M). Behind the Mach node a contact discontinuity (C) is formed between the reflected shock and the Mach stem.

The corresponding two-dimensional Riemann problem is shown in Fig. 3.2. We move to a frame where the node is at rest and denote the states as indicated. The contact discontinuity has a jump in density and tangential velocity across it. Each state is given by the two components of velocity $\vec{q}$, the density $\rho$, and the pressure $p$. Given the state in one sector, the Rankine-Hugoniot conditions determine a one parameter family of states that can occur across a shock or contact discontinuity in a neighboring sector. These conditions may be written as follows [2, pp. 301-302 and 329]:

$$\frac{p_i - p_j}{\rho_j} = \vec{q}_j \cdot (\vec{q}_j - \vec{q}_i)$$

for

$$(i,j) \in \{(0,1), (1,0), (1,2), (2,1), (0,3), (3,0)\}, \tag{3.1}$$

$$\frac{p_i}{p_j} = \frac{\mu^2 - \frac{\rho_i}{\rho_j}}{\mu^2 \frac{\rho_i}{\rho_j} - 1}$$

for

$$(i,j) \in \{(1,0), (3,0), (2,1)\}, \tag{3.2}$$

$$\vec{q}_2 \times \vec{q}_3 = 0, \tag{3.3}$$

and

$$p_2 = p_3. \tag{3.4}$$

Here $p$ is the pressure, $\vec{q}$ is the fluid velocity, and $\mu^2 = \frac{\gamma - 1}{\gamma + 1}$, where $\gamma$ is the polytropic gas constant. Relations (3.1) and (3.2) are the Rankine-Hugoniot conditions for a shock, while relations (3.3) and (3.4) express the existence of a contact discontinuity.

There are eleven equations in sixteen unknowns. From the point of view of an experimentalist, the initial conditions in a shock tube experiment, viz. four parameters specifying the density and pressure scales and the strength and orientation of the incident shock, are not sufficient to determine the solution. For this reason it could be stated that there is a missing equation for the Mach interaction. However, this missing equation is only an absence of an analytic or closed form solution to give the node trajectory on the basis of equations (3.1)–(3.4), and does not indicate an incompleteness of the Cauchy

problem for the Euler equations. From a mathematical point of view there is no missing equation, since the solution from the previous time step provides complete Cauchy data.

The front tracking problem is to obtain a complete Riemann problem solution for given Cauchy data and to select the Mach node out of that solution. As formulated this problem is too difficult. Hence we proceed with equations (3.1)−(3.4). With sixteen state variables and eleven equations at the node, we see that the Mach node lies in a five-dimensional manifold within the space of states $u_0$, $u_1$, $u_2$, and $u_3$. In lieu of solving a full two-dimensional Riemann problem to select a point in this manifold, five of the above sixteen parameters are selected to specify the node. Using physical intuition, we selected five parameters from the complete set of Cauchy data [4]. Based on numerical evidence, we believe this method does a satisfactory job of picking out the Mach node from the waves emanating from the complete solution of a two-dimensional Riemann problem that is close to a Mach node.

We compared the numerical solution for the nonsteady Mach reflection with experiments in [3]. In the experiment an incident shock with a Mach number 2.03 impinges on a wedge with angle 27°. The calculations were initialized just after the Mach configuration has appeared. The reflected shock and the Mach stem then enclose a region of about one mesh interval in height. After the bubble enclosed a region several mesh intervals in height the solution had settled down to its self-similar form as seen in the experiment. In Fig. 3.3 the constant density contours are shown. In Fig. 3.4 the wall density distribution obtained in our calculation is superimposed on the experimental data. However the calculation is preliminary in two respects. The present form of the algorithm for the propagation of the Mach triple point seems to be stable only when the initial oblateness is chosen near the experimentally determined value. Moreover the algorithm for the propagation of the point of intersection of the contact discontinuity with the wall is discernably unstable: the fluid velocity at this point is very sensitive to the pressure upstream, so the end of the contact tends to curl up. The causes of these instabilities have not yet been determined.

## 4. The Classification of Two Dimensional Elementary Waves

In this section we classify the elementary waves for two-dimensional gas dynamics. Front tracking employs a normal and a tangential operator splitting at jump surfaces and a solution of two-dimensional Riemann problems at the point singularities formed by the intersection of jump surfaces ("nodes"). An example of such a two-dimensional Riemann problem was described in the previous section. For two-dimensional compressible gas dynamics there are only a small number of such nodes.

We make some general assumptions that idealize the problem, but which we believe apply to a generic set of possible point singularities formed by the meeting of jump surfaces and centered rarefaction waves. Then we refine these general assumptions into a precise mathematical formulation, and using the latter, derive a classification scheme for

the allowed point singularities.

Excluded from this classification scheme are point singularities formed by centered waves (implosions) and points in a neighborhood of which the solution is not piecewise smooth.

**Definition 4.1** A *pressure wave* is a shock wave or a centered rarefaction wave. A *wave* is either a pressure wave or a contact discontinuity. A *node* is the point singularity formed by the intersection of waves. A rarefaction wave centered at a node is called an *incoming (forward facing) rarefaction wave* if its straight line $C^+$ or $C^-$ characteristics, in the frame in which the node is stationary, point towards the node. A shock wave emanating from a node is said to be an *incoming shock wave* if, in the stationary frame, it turns the flow towards the node. Similarly we define an *outgoing rarefaction wave* and an *outgoing shock wave*. We observe that every pressure wave at a node is either incoming or outgoing.

**Assumption 4.2.** We assume our solution $u$ to be an *elementary wave*, which, in general terms, satisfies the following:

4.2.1 $u$ is a stationary solution of the Euler equations for a polytropic gas: $u_t = 0$ and $\nabla \cdot \vec{f}(u) = 0$;

4.2.2 $u$ has the form

$$u = u_j \text{ for } \theta_{j-1} < \theta < \theta_j, \quad j = 1, \ldots, n$$

where $\theta_n = \theta_0 + 2\pi$ and each $u_j$ is constant or a centered rarefaction wave;

4.2.3 the only jumps allowed in $u$ are shock waves and contact discontinuities;

4.2.4 $u$ is generic;

4.2.5 $u$ is an entropy increasing solution, with

$$u = \lim_{\nu \to 0} u^\nu,$$

where $u^\nu$ is a solution of the Navier-Stokes equations with viscosity $\nu$.

First consider all possible elementary waves containing only contact discontinuities. If one of the sectors has a 180° opening, there can be a nonzero discontinuity in the tangential velocity across its boundary. All other contact discontinuities contain only temperature jumps. It is possible for any number of them to occur, and at any set of angles.

From now on assume that the elementary wave contains at least one pressure wave. Assumptions 4.2.4 and 4.2.5 are not written in mathematical terms, so we formulate the ideas that they express in a manner that we can use in our analysis.

4.2.4a No incoming rarefaction waves are allowed. There can be at most two incoming pressure waves, which are necessarily shock waves. If the flow on the ahead side (the side with the lower pressure) of an incoming shock wave is adjacent to a contact discontinuity that is within 90° of the incoming shock,

only this one incoming shock wave is allowed.

4.2.5a No sectors of zero velocity bounded by contact discontinuities ("embedded wedges") are allowed.

Observe that the elementary waves that satisfy 4.2.1 through 4.2.4 but fail to satisfy 4.2.5a can be interpreted as solutions of an initial/boundary-value problem if the contact discontinuities bounding the embedded wedge are replaced with reflecting walls.

In [4] we have determined that an elementary wave containing a pressure wave is restricted by the following. There is a unique streamline through the node. There is either one or two incoming shock waves. There is no more than one outgoing pressure wave on each side of the streamline leaving the node, only one of which may be a rarefaction. The streamline is a contact discontinuity if there are two outgoing pressure waves. This then leaves us with only a small number of possible elementary waves, which we shall determine presently.

**Theorem 4.3.** Under Assumptions 4.2 an elementary wave containing at least one pressure wave is one of the following types, as specified in detail below: cross, overtake, Mach, diffraction, and transmission.

What follows is an explanation of the types together with figures. For a proof of the theorem see [4].

**Diffraction.** The diffraction of a shock impinging on a contact discontinuity, causing a reflected and a transmitted shock is a possible solution, see Fig 4.1.a. We show in Fig. 4.1.b how the solution may be constructed by drawing the appropriate shock polars in the $\theta, p$ plane.

**Diffraction.** The configuration in Fig. 4.2.a is an elementary wave. It is as in Fig. 4.1.a, but with a rarefaction wave in place of a reflected shock. The solution is constructed using shock polars, as indicated in Fig. 4.2.b.

**Transmission.** A shock impinging on a contact discontinuity and causing a transmitted shock but no reflected wave (see Fig. 4.3.a) is a possible elementary wave; see the corresponding shock polar in Fig. 4.3.b.

**Mach node.** A direct Mach reflection, where the incident shock breaks into two shocks, the reflected shock and the Mach stem, is a possible elementary wave; see Fig 4.4.a. The solution is found using shock polars as in Fig 4.4.b.

**Overtake.** It is possible to have two incoming shocks overtake each other and give rise to two outgoing shocks separated by a contact discontinuity (see Fig. 4.5.a). The solution may be constructed using shock polars as in Fig. 4.5.b. The special case where one of the two incoming shocks has zero strength coincides with the Mach node case.

**Overtake.** One shock may overtake the other, resulting in a reflected rarefaction and a transmitted shock (see Fig 4.6.a). The solution is found using shock polars as in Fig. 4.6.b. Note that for the same parameters of the two incident shocks, both this case and the previous case are possible.

**Cross or Mach node.** Two incident shocks colliding to form two reflected shocks separated by a streamline (see Fig. 4.7.a) is a possible elementary wave. The solution is found using shock polars as in Fig. 4.7.b. The special case of one incident shock having zero strength gives the direct Mach node. A single shock wave in the outgoing sector defines the inverted Mach node; this interaction is a limit of the cross case above, where the shock between region 2 and 3 in Fig. 4.7.a reduces to zero.

## 5. Some Problems and Conjectures Concerning Riemann Problems

In this section we drop the restriction to two dimensions and to gas dynamics, but we retain the terminology of Sec. 4. Recall that in steady supersonic two-dimensional gas dynamics, where the direction of the flow defines a timelike direction, the equations can be reduced to the form of a one-dimensional time-dependent system of conservation laws. Then the two-dimensional elementary waves viewed in the stationary frame are Riemann problems for a distinct but related one-dimensional system. Similarly Riemann problem solutions in $n-1$ space dimensions are qualitatively similar to elementary waves in $n$ dimensions.

We list some problems of general interest in this area.

1. The possible $n$-dimensional elementary waves for a system of conservation laws could be classified. The elementary waves in two-dimensional polytropic gas dynamics were classified in the previous section.

2. Let the incoming wave operator be the solution operator bringing two or more elementary waves to a single point and thereby defining a Riemann problem. The outgoing wave operator also acts on single elementary waves by mapping to the configuration at a time of bifurcation, or dynamic instability; this also defines a Riemann problem. The range of this operator is limited to the possible mergers or bifurcations of the elementary waves found in the classification above. Can this range be categorized?

3. The outgoing wave operator gives the possible elementary waves that may occur in the solution of the Riemann problems in the range of the incoming wave operator. We pose the question of existence of solutions for this restricted set of data. Are solutions piecewise smooth, so that there is a finite number of outgoing elementary waves? The answer depends on the order of the system, the dimension of space, and the convexity or number of inflection points in the flux function, as examples [6] show and analogies [7] suggest.

4. A logical scattering matrix $S$ is a map from sets of incoming wave types to sets of outgoing wave types as labeled by the solutions to problem 1. It decides which types of incoming waves produce which types of outgoing waves. In the language of quantum mechanics, the problem here is to classify the possible $S$ matrix graphs. Let us consider this problem from the point of view of two-dimensional gas dynamics. We restrict attention to Riemann data contained in the range of the incoming wave operator as defined in 2 above. Under such restriction, the waves will be said to be in incoming

order. The allowed nodes of Sec. 4 provide interchange of wave order to an outgoing order. In general, however, the interchange of wave order produces three outgoing waves from two incoming waves and need not reduce the total number of wave pairs that fail to be in outgoing order. On this basis, we expect that even simple incoming configurations could produce complicated outgoing wave interactions. It is possible that the complication (e.g. the number of nodes), while not bounded *a priori*, is still finite. In fact the wave interactions typically decrease the Mach number of the flow, and may give rise to a subsonic region, inside of which no pressure waves can occur. Related to this possibility is the occurrence of nodes with only two outgoing waves. Such nodes allow the interchange of wave order with a reduction in the total number of pairs that are out of order.

5. Uniqueness is an open problem. Well known problems of nonuniqueness are not understood on a fundamental level. For example, consider an incident shock hitting a wedge, resulting in either a regular reflection or Mach reflection. There are regions where both solutions are possible. By introducing additional physical effects such as viscosity, with a resulting boundary layer, or surface roughness on a certain length scale, this overlapping region of nonuniqueness might disappear.

6. Extended or nonlocal Riemann problems may be considered, where the restriction of constancy in sectors between the waves is replaced by linear or higher order data. This has been implemented for one dimension in the normal propagation of the front [1].

7. Lower order terms in the equations and new waves in the Riemann solution may be caused by geometrical effects and by external sources.

8. The geometry in the large defined on the state space by the flux function needs to be understood. For gas dynamics the qualitative behavior of solutions may be studied by considering the acoustic waves of the linearized problem. But this is not the case for all hyperbolic conservation laws, and new families of waves may be possible in the large. The topology defined by the critical points of the flux function $f$ in (1.1) is important here. A critical point is a point in state space where the gradient $A = \nabla f$ has coinciding eigenvalues. At the critical points equation (1.1) is no longer strictly hyperbolic; moreover $A$ can fail to have a complete set of eigenvectors. Such a loss of strict hyperbolicity is not pathological in applications, and the mathematical consequences of this fact have not been developed. An extension of this phenomena are the problems for which the equations in different regions of state space change type. The applications are of general interest: oil reservoir simulation, transonic flow in gas dynamics, chemically reacting flows, and nonlinear elasticity.

**Acknowledgements**

We thank Jonathan Goodman for helpful discussions.

**References**

1. I-L. Chern, J. Glimm, O. McBryan, B. Plohr, and S. Yaniv, "Front Tracking for Gas Dynamics," Submitted to J. Comp. Phys., 1984.
2. R. Courant and K. Friedrichs, *Supersonic Flow and Shock Waves*, Interscience, New York, 1948.
3. R. Deschambault and I. Glass, "An Update On Non-Stationary Oblique Shock-Wave Reflections: Actual Isopycnics and Numerical Experiments," *J. Fluid Mech.*, vol. 131, pp. 27-57, 1983.
4. J. Glimm, C. Klingenberg, O. McBryan, B. Plohr, D. Sharp, and S. Yaniv, "Front Tracking and Two Dimensional Riemann Problems," *Adv. Appl. Math.*, 1984. To appear.
5. J. Guckenheimer, "Shocks and Rarefactions in Two Space Dimensions," *Arch. Rational Mech. Anal.*, vol. 59, pp. 281-291, 1975.
6. B. Lindquist, "The Two Dimensional Scalar Riemann Problem," New York University Preprint, 1984.
7. J. Rauch and M. Reed, "Jump Discontinuities of Semilinear, Strictly Hyperbolic Systems in Two Variables," *Comm. Math. Phys.*, vol. 81, pp. 203-227, 1981.
8. D. Wagner, "The Riemann Problem in Two Space Dimensions for a Single Conservation Law," *J. Math. Anal.*, vol. 14, pp. 534-559, SIAM J. Math. Anal., 1983.

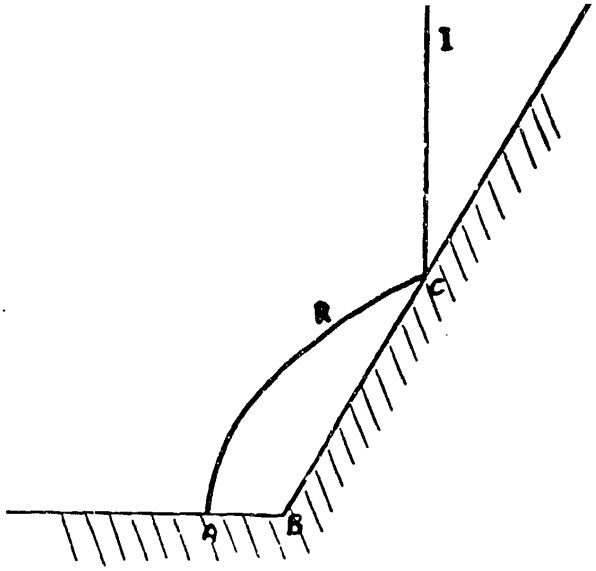


**Fig. 2.1.** Regular reflection of a shock wave by a wedge. A vertical shock *I* has struck a 63° wedge from the left, causing a reflected shoc *R*, which forms a bowshock in front of the wedge.

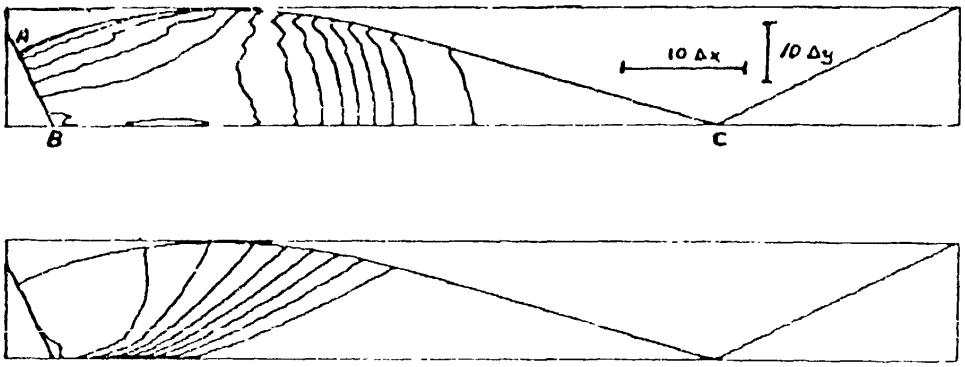


**Fig. 2.2.** The numerical simulation of a regular reflection, where the incident shock has Mach number 2.05 and the wedge angle is 63.4°. The calculation was performed on a 80 by 20 grid. The top picture shows the lines of constant density inside the bubble formed by the reflected shock. The bottom picture shows the lines of constant entropy. They should coincide with the integral curves for the self-similar velocity field. Theoretical arguments in the text suggest that these integral curves all terminate at the corner.

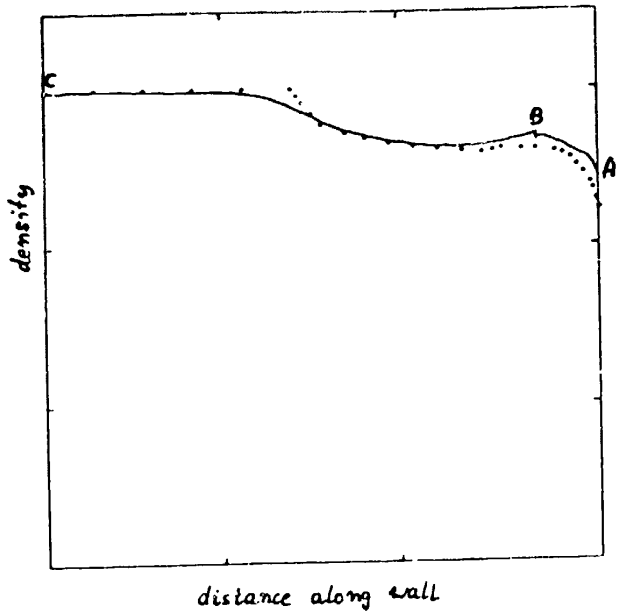


**Fig. 2.3.** The computed (solid line) density distribution along the wall for the regular reflection run compared to the data obtained in the experiments of Deschambault and Glass (dots).

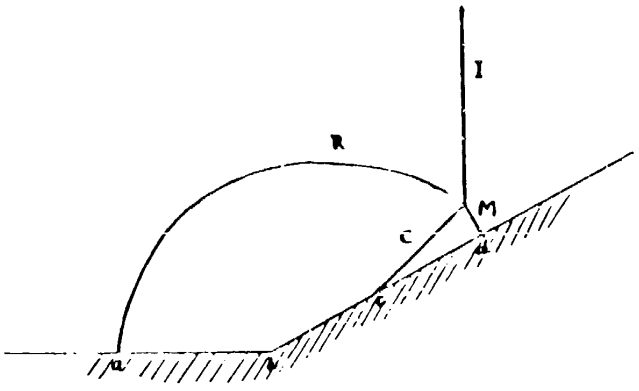


**Fig. 3.1.** Mach reflection of a shock wave by a wedge. A vertical shock $I$ has struck a 27° wedge from the left. The point where the incident shock $I$ and reflected shock $R$ meet is connected to the wall by a shock called a Mach stem ($M$). Behind the triple point, where the three shocks meet, a contact discontinuity $C$ is formed between the reflected shock and the Mach stem.

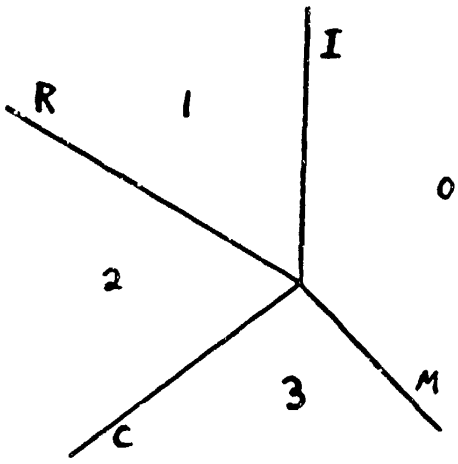


**Fig. 3.2.** The Riemann problem corresponding to the triple point obtained in a Mach reflection. We assume the shocks and contact discontinuities are straight lines (labeled as in Fig. 3.1) with constant states 0 through 3 in the wedges.

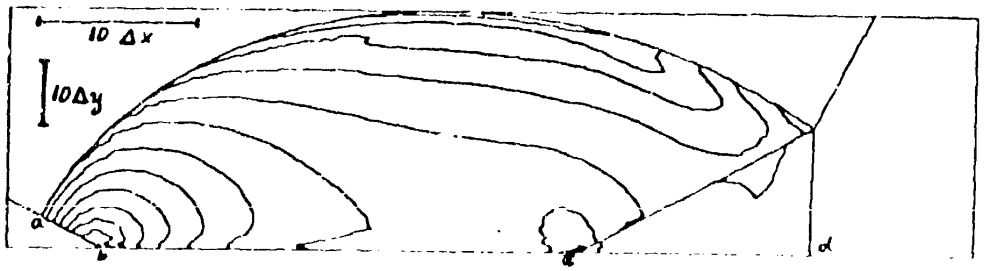


**Fig. 3.3.** The numerical simulation of a Mach reflection, where the incident shock has Mach number 2.03 and the wedge angle is 27°. Inside the bubble formed by the reflected shock we show the calculated lines of constant density. The calculations were performed on a 60 by 40 grid.

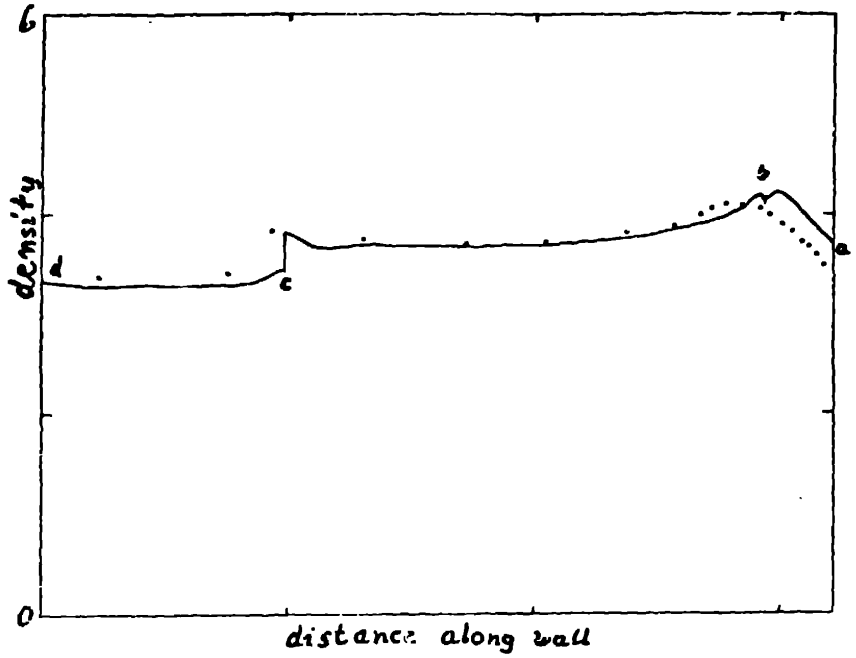


**Fig. 3.4.** The density distribution along the wall of the Mach reflection run (solid line) shown superimposed on the data found experimentally by Deschambault and Glass (dots).

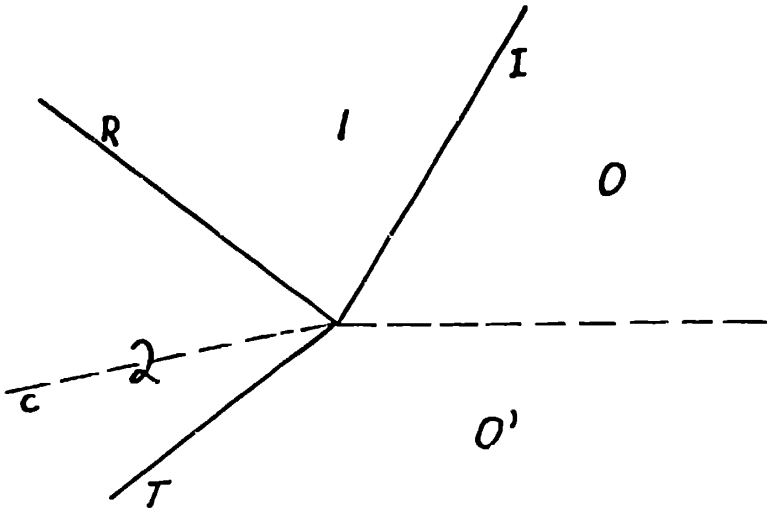


**Fig. 4.1.a. Diffraction. A shock *I* can diffract through a contact discontinuity *C* to cause a reflected shock *R* and a transmitted shock *T*.**

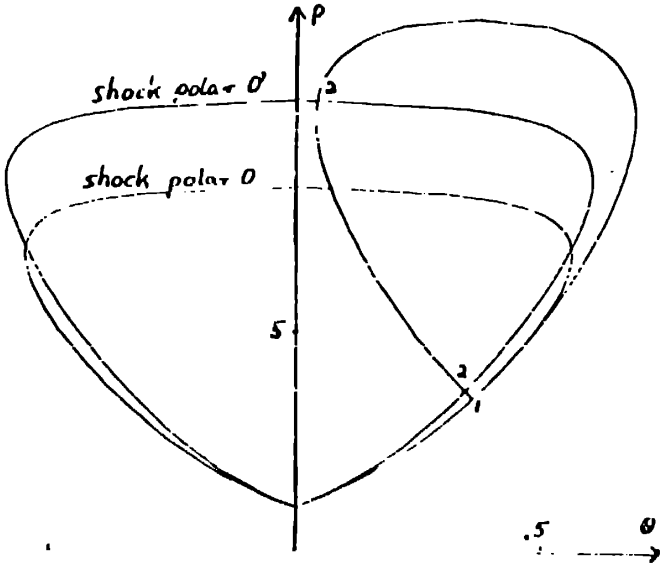


**Fig. 4.1.b. The shock polars corresponding to Fig. 4.1.a. The Mach number of state 0 is 2.7 and that of state 0' is 3. The shock strength of *I* is 3.**

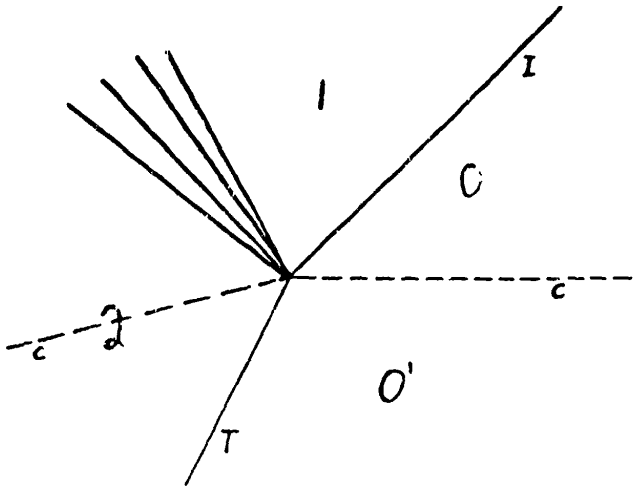


**Fig. 4.2.a.** Diffraction. The diffraction of a shock $I$ by a contact discontinuity $C$ can cause a reflected rarefaction wave $R$ and a transmitted shock $T$.

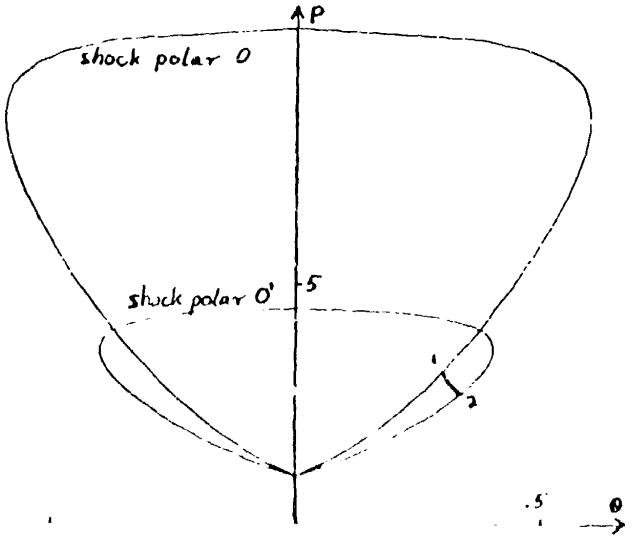


**Fig. 4.2.b.** The shock polars corresponding to Fig. 4.2.a. The Mach number of state 0 is 3 and that of state 0' is 2. The image of a 1'–characteristic in this $p$ , $\theta$ plane is drawn, connecting the states $p = 3$ on one shock polar to $p = 2.8$ on the other.

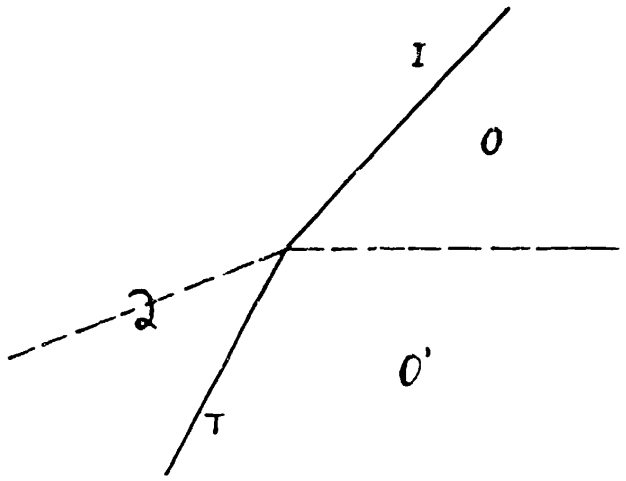


**Fig. 4.3.a.** Transmission. A shock *I* incident on a contact discontinuity *C* causing a transmitted shock T but no reflected wave is possible.

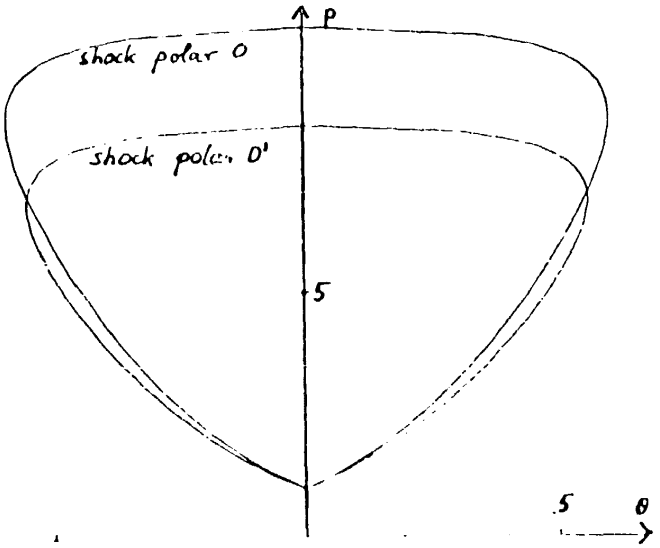


**Fig. 4.3.b.** The shock polars corresponding to Fig. 4.3.a are shown. The Mach number of state 0 is 3 and that of state 0' is 2.7.

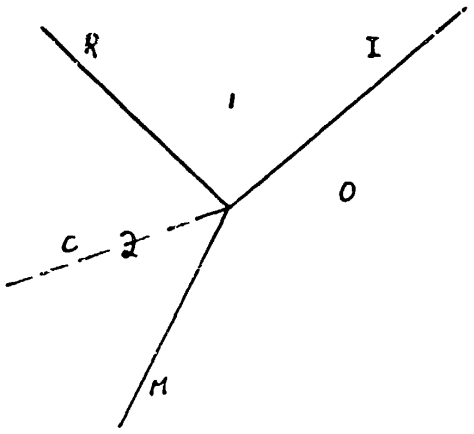


**Fig. 4.4.a.** Mach node. Direct Mach reflection is shown, with the incident shock *I* breaking into a reflected shock *R* and a Mach stem *M* separated by a contact discontinuity *C*.

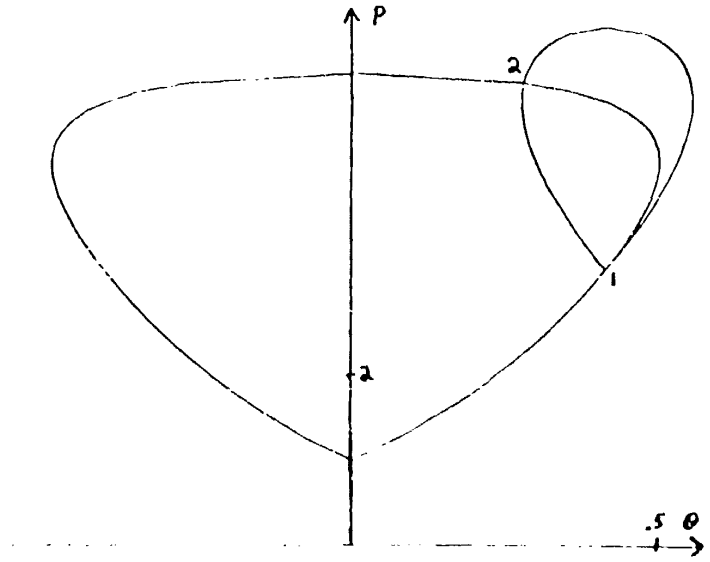


**Fig. 4.4.b.** The shock polars corresponding to Fig. 4.4a. The Mach number of state 0 is 2.2 and the shock strength of *I* is 3.2.

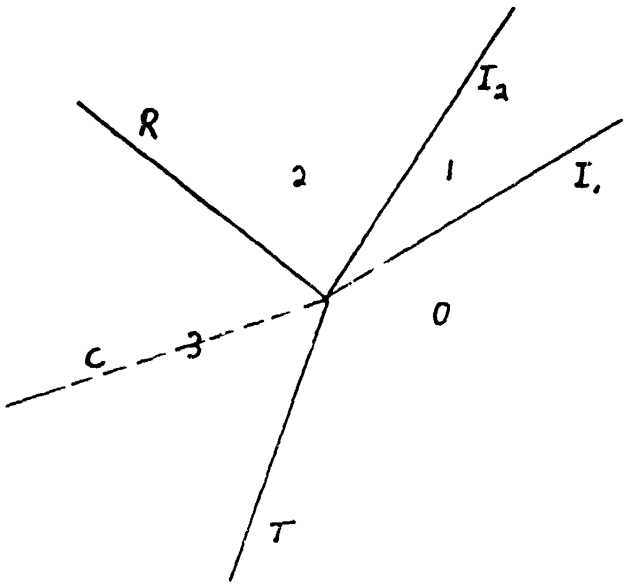


**Fig. 4.5.a.** Overtake. It is possible to have one incoming shock $I_1$ overtake another $I_2$ to cause a reflected shock $R$ and a transmitted shock $T$ with a contact discontinuity $C$ between them.

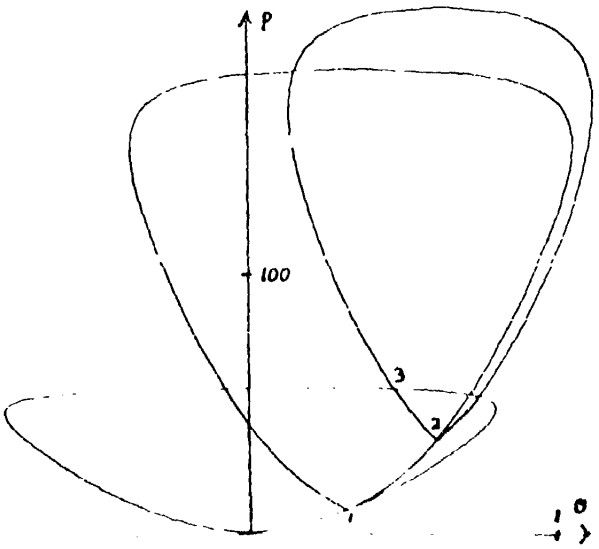


**Fig. 4.5.b.** The shock polars corresponding to Fig. 4.5.a. The Mach number of state 0 is 7, the shock strength of the incident shock $I_1$ is 9.5, and the shock strength of $I_2$ is 3.9.

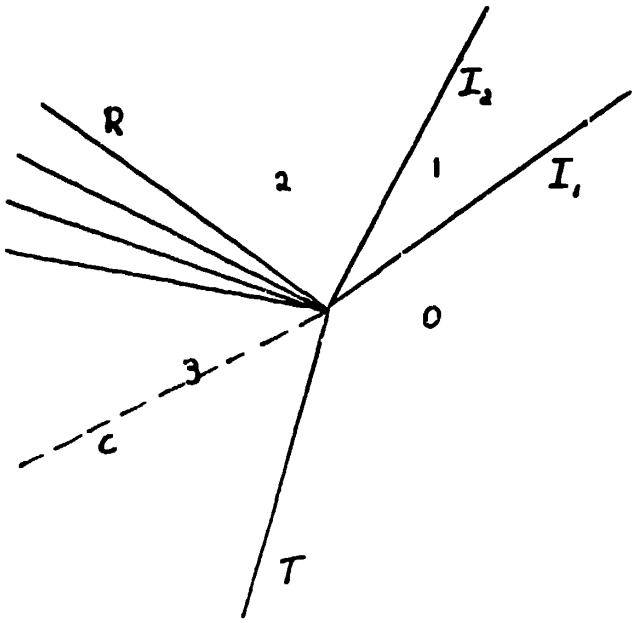


**Fig. 4.6.a. Overtake.** It is possible for one incoming shock $I_1$ to overtake another $I_2$ to cause a reflected rarefaction wave and a transmitted shock wave separated by a contact discontinuity.

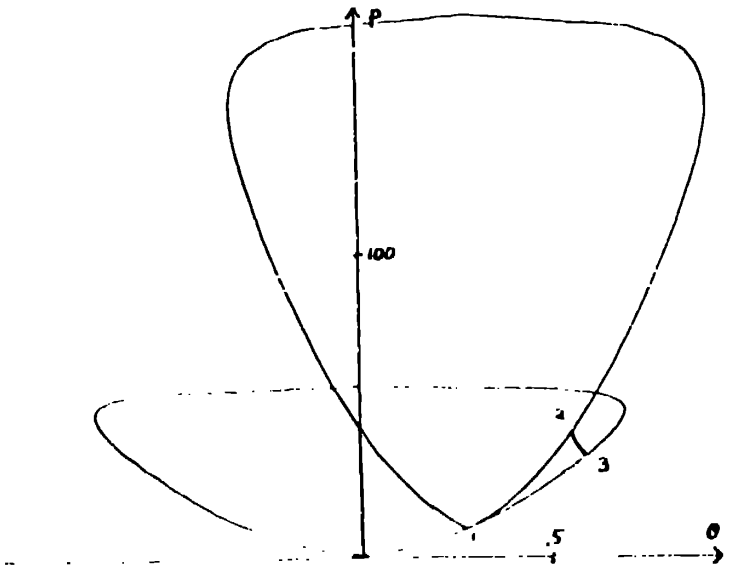


**Fig. 4.6.b.** The shock polars corresponding to Fig. 4.6.a. The Mach number of state 0 is 7, the shock strength of the incident shock $I_1$ is 9.5, and the shock strength of $I_2$ is 3.9.

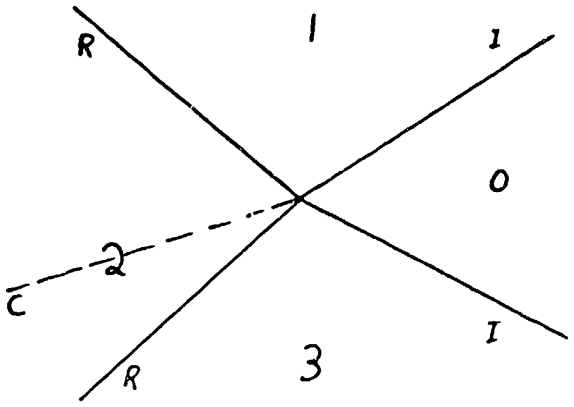


**Fig. 4.7.a.** Cross. Two may shocks collide and cause two reflected shocks separated by a contact discontinuity.

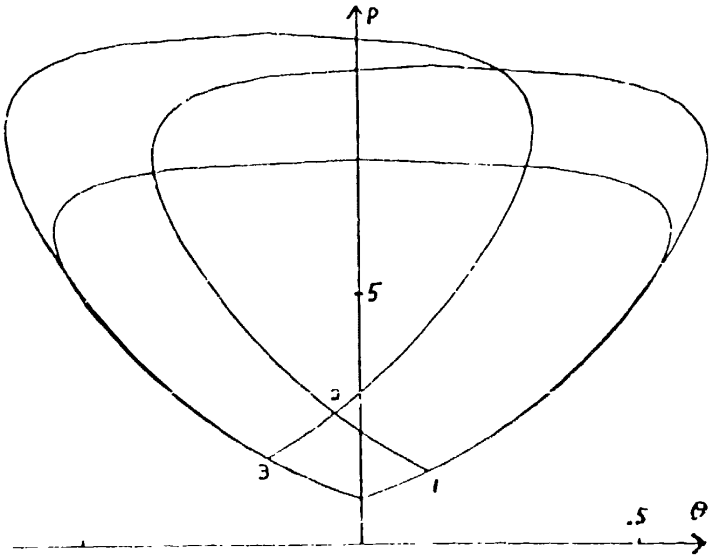


**Fig. 4.7.b.** The shock polars corresponding to Fig. 4.7.a. The Mach number of state 0 is 2.7 and the shock strengths of the incident shocks are 1.6 and 1.9.